

# Vacuum pressure generation via microfabricated converging-diverging nozzles for operation of automated pneumatic logic

Theodore Christoforidis<sup>a</sup>, Erik M Werner<sup>b</sup>, Elliot E Hui<sup>b</sup>, David T Eddington<sup>a\*</sup>

a. Department of Bioengineering, University of Illinois at Chicago, Chicago, Illinois, 60607, USA

b. Department of Biomedical Engineering, University of California, Irvine, CA, 92697, USA

\*To whom correspondence should be addressed. E-mail: dte@uic.edu

## Abstract

Microfluidic devices with integrated pneumatic logic enable automated fluid handling without requiring external control instruments. These chips offer the additional advantage that they may be powered by vacuum and do not require an electricity source. This work describes a microfluidic converging - diverging (CD) nozzle optimized to generate vacuum at low input pressures, making it suitable for microfluidic applications including powering integrated pneumatic logic. It was found that efficient vacuum pressure was generated for high aspect ratios of the CD nozzle constriction (or throat) width to height and diverging angle of  $3.6^\circ$ . In specific, for an inlet pressure of 42.2psia (290.8kPa) and a volumetric flow rate of approximately 1700sccm, a vacuum pressure of 8.03psia (55.3kPa) was generated. To demonstrate the capabilities of our converging - diverging nozzle device, we connected it to a vacuum powered peristaltic pump driven by integrated pneumatic logic and obtained tunable flow rates from 0 to 130  $\mu\text{L}/\text{min}$ . Finally, we demonstrate a proof of concept system for use where electricity and vacuum pressure are not readily available by powering a CD nozzle with a bicycle tire pump and pressure regulator. This system is able to produce a stable vacuum sufficient to drive pneumatic logic, and could be applied to power automated microfluidics in limited resource settings.

## Introduction

A converging-diverging nozzle is a fundamental fluid dynamics principle broadly used in the macroscale, mostly as a flowmeter. For incompressible fluids it is named as a Venturi nozzle, while for compressible fluid applications it is more accurately termed as a de Laval nozzle. Here we will simply use the term converging-diverging (CD) nozzle. At the microscale, the CD nozzle has been applied as a regulator for liquid flows (Chang et al., 2007, 2010), for liquid aspiration devices (Perdigones et al., 2010), as a sampling tool for gastrointestinal fluids (Koo et al., 2011), for transdermal extraction of interstitial fluid for glucose monitoring (Li et al., 2013), or as a portable mass spectrometer (Curtis et al., 2012). In a previous study, Yu et al. (Yu et al., 2012) fabricated an optimized micro-Venturi nozzle to investigate its

capacity for vacuum generation, and acquired a maximum vacuum pressure of 86kPa (~12.5psia) when an external pressure of 240kPa (34.8 psia) was applied. While these results were sufficient for their application, a greater vacuum from a smaller input pressure would expand the usefulness of the CD nozzle on the microscale.

Here, we describe an optimized microfluidic CD nozzle capable converting a moderate positive pressure, such as that generated by a bicycle tire pump, into vacuum pressure powerful enough to drive microfluidic logic. Automated microfluidic devices usually depend on electrical power and bulky external instruments to meet pumping, valving, and timing requirements. Microfluidic logic circuits offer an alternative allowing controllers to be built on-chip that reduce or eliminate the need for off-chip flow control components, and do not require electrical power to operate. Previously, autonomous microfluidic devices have been demonstrated that leverage microfluidic logic to achieve peristaltic pumping (Duncan et al., 2013) or multi-step fluid handling operations (Nguyen et al., 2012). The logic gates of these devices were implemented using normally-closed pneumatic membrane valves first demonstrated by the Mathies group (Grover et al., 2003, 2006; Jensen et al., 2007) and require only a steady supply of moderate vacuum pressure to operate. While a stable vacuum source is widely available in a lab setting or readily generated with a vacuum pump, these resources may not always be available to users in limited resource settings and a solution could be to generate vacuum on chip with a CD nozzle.

After our optimization of the CD nozzle, we demonstrate vacuum generation equaling previously reported designs at much lower input pressure as well as the ability to generate vacuum pressure as great as 8.03 psia (Figure 1). To demonstrate an application of the additional vacuum produced by our design, we integrated our micro fabricated CD nozzle with a peristaltic pump device driven by microfluidic digital logic (Duncan et al., 2013). The possible applications of our enhanced design could extend to many more devices, including those currently powered by vacuum pumps or syringe pumps. Finally, we suggest a very simple model system in which a bicycle tire pump and a pressure regulator are used to generate a stable positive pressure input to our CD nozzle. This system provides an obtainable and widely available source of power that can be used to drive automated microfluidic devices in resource limited settings.

## Methods and Materials

### Microfabrication

#### Micro fabricated CD nozzle devices

CD nozzles were fabricated using standard soft lithography technique. In brief, SU-8 was spun onto a silicon wafer and selectively exposed to UV light using a photomask (Fineline Imaging, Colorado Springs, CO) to form a negative master mold. Polydimethylsiloxane (PDMS) elastomer (Sylgard 184, Dow Corning, Midland, MI) was mixed in a 10:1 ratio (w/w), poured on top of the patterned silicon master, degassed for 1 hour and then cured at 85° C for two hours. After, PDMS devices were peeled from the mold and 2.1 mm holes were punched using needles for inlets and outlets. The elastomer layer was bonded to a glass microscope slide via corona plasma treatment and heated at 85° C for 1 hour while applying a weight of 0.5kg. This produced a strong seal and the resulting devices sustained pressures over 50psig without failing.

#### Autonomous pump fabrication

The microfluidic pneumatic logic circuits used in this study were composed of a thin elastomeric sheet sandwiched between two patterned layers of polymethyl methacrylate (PMMA). Detailed fabrication steps have been previously described (Duncan et al., 2015). In brief, channel geometry was designed using commercially available CAD software (AutoCAD, Autodesk, San Rafael, CA), and machined into a 1/16" thick sheet of PMMA (McMaster Carr 8560K171). PDMS sheets with a thickness of 254 μm (HT-6240, Rogers Corp, Rogers CT) were used as the elastomeric membrane. Via holes were patterned onto the PDMS sheets using a 25W CO<sub>2</sub> laser (VLS2.30, Universal Laser Systems, Scottsdale AZ) to connect channels on opposite sides of the chip. Prior to chip assembly, all device layers were cleaned thoroughly using distilled water and 100% isopropyl alcohol followed by drying with compressed air. Layers were manually aligned under a stereoscopic microscope, clamped together using glass slides and binder clips, and annealed at 110°C for 1 hour to ensure the device was sealed.

### Experimental Setup

External pressure was supplied to the microfluidic CD nozzle via a nitrogen tank connected through 1/16" ID Tygon tubing and luer lock connections (Cole-Parmer, Vernon Hills, IL). A miniature pressure regulator (EW-68826-50, Cole-Parmer, Vernon Hills, IL) or a glass tube rotameter (Omega Engineering, Inc., Stamford, CT) was used to adjust the inlet pressure.

## Data Acquisition

Pressure measurements were obtained using pressure sensors (Honeywell 40PC100G2A for positive and Honeywell 40PC015V2A for negative pressure) connected to a data acquisition device (NI 9205, National Instruments, Austin, TX) and sampled at 20Hz using LabVIEW software (National Instruments, Austin, TX). For volumetric flow rate measurements, two electronic flowmeters were used (FMA-2306 OMEGA Engineering and AWM5101VN Honeywell Inc.) in place of the pressure sensors. The pressure data were obtained in a continuous fashion by slowly adjusting the inlet pressure using a rotameter or a pressure regulator. Experiments were repeated three times for three different devices, data was analyzed with MATLAB (MathWorks, Inc.) and is presented as the mean with error bars of standard deviations.

## Results and Discussion

### Micro fabricated CD nozzle optimization

A CD nozzle is a device that allows vacuum pressure to be generated via the device geometry rather than relying on moving parts (Figure 1a). Air enters the nozzle through the inlet and passes through a converging section where the channel walls narrow until they reach their point of maximum constriction, known as the vena contracta or throat. As the pressure increases in the convergent part, the pressure on the throat decreases i.e. a negative pressure is generated. This is attributed to the induced high pressure on the inlet which forms a jet flow through the throat. This jet flow expands in the divergent part where the pressure is increased and the flow can be either subsonic or supersonic. The momentum of the jet induces shear stresses on the boundaries of the divergent nozzle which force the surrounding fluid mass inwards (Bird, 2002).

For compressible fluids, increasing the pressure applied at the inlet will increase the flow rate and increase the vacuum generated at the throat of the device until the fluid velocity at the throat reaches the speed of sound (Mach number equal to 1). At this point the mass flow rate reaches its maximum value and the flow is choked. Thus, the occurring jet does not gain any momentum if the inlet pressure is further increased, and further decrease in the negative pressure is not possible. In addition, for supersonic flows in the divergent part there is a certain inlet pressure range where shock waves on the flow occur (Shapiro, 1953).

Moreover, on the scale that the devices are fabricated, the shear forces are not negligible and the flow can become highly resistive, limiting the momentum of the occurring jet flow. The electrical analogy of the resistance of a duct is given by

$$\Delta p = Q \times R$$

Where  $R$  is related inversely to the cross section of the duct where for rectangular cross sections is given by

$$R = \frac{h \times w}{h + w}$$

Where  $h$  is the height and  $w$  is the width of the microchannel(Kirby, 2010). Therefore, it is expected that for the same inlet pressure, higher flow rates would be obtained for larger cross sections.

In addition, our devices are fabricated with an elastomeric material which deforms with increasing pressure. Therefore, the cross section is increased with increasing pressure. An exact formula that describes the cross section change due to the deformability of PDMS has only been investigated for liquids(Gervais et al., 2006). The deformability of PDMS when induced in pressure from gases has not been investigated yet and is out of the scope of this work in which we used experimental optimization of device parameters to study the result of negative pressures generated.

A	3.7mm	E	2.2mm
B	3mm	F	28mm
C	1mm	a	40°
D	2mm		

**Table 1.** Fixed dimensions of the micro fabricated CD nozzle as shown in Figure 1.

For all cases that we studied, we fixed the dimensions as shown in Table 1, and investigated three parameters: the channel height  $h$ , the angle of the divergent nozzle  $b$ , and the throat width  $w$ . In Figure 2, we observed that when the height of the device is small, the CD nozzle produced very little vacuum, an effect that was also observed by Chang et al. (Chang et al. 2007) where there vacuum pressure was not obtained for heights below 80 $\mu$ m. This is attributed to the high channel resistance, causing the momentum of the jet flow to be shear stress limited at the throat. This phenomenon is shown in Figure 2a, where a weak vacuum is produced only for the larger diverging angles (3.6° and 7°) and for high inlet pressure (>30psia). Additionally, in Figure 2c, d, and e it is observed that little vacuum (12-13psia) is

produced for small angles ( $2.2^\circ$  and  $2.7^\circ$ ), however for a diverging angle of  $3.6^\circ$  the vacuum increases significantly for inlet pressures in the range of 30-40psia. For the  $7^\circ$  divergent angle higher inlet pressures (50-55psia) are required in order to acquire the greatest amount of vacuum. We attribute this to jet expansion occurring farther away from the throat. As the flow exits the constricted area of the throat, a jet is formed which expands perpendicular to the throat axis. For low diverging angles the expansion of the jet is compressed and momentum is lost. For higher angles the jet expands properly and higher input flows are required to reach the minimum negative pressure. Thus, for the purpose of generating a large vacuum pressure from moderate input pressure, we selected a  $3.6^\circ$  diverging angle for further nozzle optimization.

Using a  $3.6^\circ$  diverging angle for the nozzle, vacuum pressure for different throat widths  $w$  were measured. For devices with sufficient height, as throat width was decreased vacuum generation improved (Figure 3). This is due to the small throat creating a jet with greater momentum at high input pressures for devices that are not highly resistive. Our optimal design with  $30\mu\text{m}$  throat width and  $500\mu\text{m}$  height was able to produce 8.03psia of vacuum at an input pressure of 42.2psia. For smaller device heights, the additional resistance along the entire length of the channel created too high a resistance to flow. Input pressures over 45 psig were required to reach peak vacuum output, and some devices failed at input pressures over 50 psig.

One interesting device combination is the case of  $30\mu\text{m}$  throat for  $150\mu\text{m}$  height where the pressure decreases slowly and an abrupt decrease occurs after 45psia. This is assumed to be due to the compressibility of PDMS where the increased cross section causes the cross section to widen. For devices of  $80\mu\text{m}$  height the resistance of the flow is very high for a high vacuum pressure to be obtained and many devices failed when the applied pressure exceeded 50psig. On most devices, the standard deviation of output pressure increased for input pressures greater than or equal to the pressure that creates optimal vacuum. There was also device-to-device variation as each device showed a different lowest negative pressure.

In addition to the inlet pressure, volumetric flow rates were acquired for each case. The vacuum pressure measured for different volumetric flow rates showed respective patterns as the vacuum for different inlet pressures for heights above  $250\mu\text{m}$ . However, for each case of width and angle of the diverging section the distribution of vacuum pressure for different inlet pressures was similar for each height (Figure S1), while the respective vacuum pressure obtained for different flow rates was different for each height, where for higher heights the required inlet flow rate increases (figure 4). Specifically, for

the geometry of throat width  $30\mu\text{m}$  and angle of  $3.6^\circ$  for the diverging part of the nozzle, that the lowest vacuum pressures were acquired, the lowest vacuum pressure was acquired in the region of flow rate of 2100sccm for device height of  $500\mu\text{m}$ , in the region of 1400sccm for device height of  $400\mu\text{m}$ , in the region of 1100sccm for device height of  $250\mu\text{m}$ , and in the region of 800sccm for device height of  $150\mu\text{m}$ . Thus, it is obvious that in order to reduce the volumetric flow rate, i.e. the consumption of used gas, the devices with smaller heights are preferred. Finally, acquiring the flow rate for each inlet pressure, it is observed that higher pressure is required for the nozzles with smaller throat cross sections in order to achieve the same flow rate (Figure S2). Additionally, the slope of this graph is correlated with the resistance of the flow in the electrical equivalent and does not follow a linear pattern due to compressibility effects.

### Autonomous pumps operated with micro fabricated CD nozzle devices

As a proof-of-concept application for the micro fabricated CD nozzle devices, the vacuum output was used to drive a autonomous peristaltic micropump. The micropump incorporated both pneumatic control circuitry and fluid handling together on-chip using normally closed membrane valves in a manner similar to previous reports (Duncan et al., 2013, Duncan 2015). When supplied with at least 2 psig of vacuum, an oscillator circuit drove liquid handling valves to open and close sequentially, creating a peristaltic pumping pattern. The pump produced flow rates from 0 to  $130\mu\text{L}/\text{min}$  that were linearly related to the vacuum generated by the micro fabricated CD nozzle ( $R^2 = 0.99$ ) (Figure 5). Much higher or lower flow rates are possible by adding additional liquid handling valves or altering the oscillator circuit to drive the valves faster or slower. While the control circuitry and liquid handling in this chip was simple, a complete microprocessor has been demonstrated using similar pneumatic membrane valves (Rhee, 2009), suggesting more complicated fluid handling operations can be readily achieved.

### Hand powered on-chip vacuum pump

In limited resource settings, the pressure required to operate our micro fabricated CD nozzle may not always be available. We demonstrate operation of the CD nozzle vacuum generation chip using a common bike pump and a pressure regulator (Figure 6a). Pumping the bike pump at a moderate stroke rate is sufficient to supply a constant inlet pressure above 50psia to the CD nozzle, which in turn generates a constant vacuum similar to previous experiments conducted using a compressed nitrogen cylinder (Figure 6b). In this way the alternating pump pressure is stabilized as soon as the pressure of the pump is higher than the outlet pressure of the pressure regulator. It is observed that the inlet pressure and the vacuum pressure maintain stable values 53.4psia in a range of 1.48psi and 9.07psia

within 0.11psi respectively for a duration of 360 seconds. In figure 6c, it is observed that if the pressure provided to the regulator is not higher than the adjusted pressure of the regulator, the outlet pressure drops below its adjusted value.

## Conclusions

An improved microfabricated CD nozzle was designed to generate strong vacuum pressure and demonstrated using microfluidics that contain integrated vacuum powered pneumatic logic. It was found that a key property of the nozzle geometry was to narrow the throat while keeping the height of the device high in order to avoid extremely high flow resistance. While fabrication of high aspect ratio devices of up to 1:20 using SU-8 is possible, devices with throat widths below 30um collapsed. The vacuum pressures obtained did not decrease linearly with increasing inlet pressure and in cases abrupt decreases were observed due to compressibility effects of the gas. In our optimal design, the maximum acquired vacuum pressure of 8.03psia (55.3kPa) was achieved for an inlet pressure of 42.2psia (290.8kPa) and a volumetric flow rate of approximately 1700sccm.

By using one of these micro fabricated CD nozzles, we were able to drive an autonomous peristaltic pump at a flow rate of up to 130 $\mu$ L/min. Pumps capable of higher flow rates or devices containing higher levels of automation are possible. Finally, a common bike pump and pressure regulator are able to provide sufficient pressure to operate the micro fabricated CD nozzle. In this system, the nozzle and the autonomous peristaltic pumps were fabricated by low cost methods, and the pressure source is low cost and readily available. In the future, a system like this could enable automated assays for limited resource settings.

## Acknowledgements

This work was supported by National Science Foundation 1253060, DTE.

## Literature

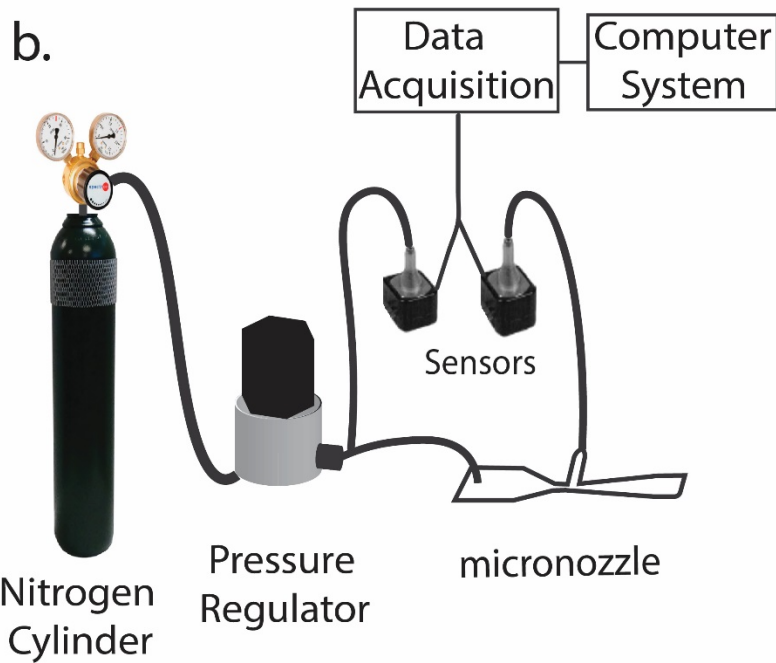
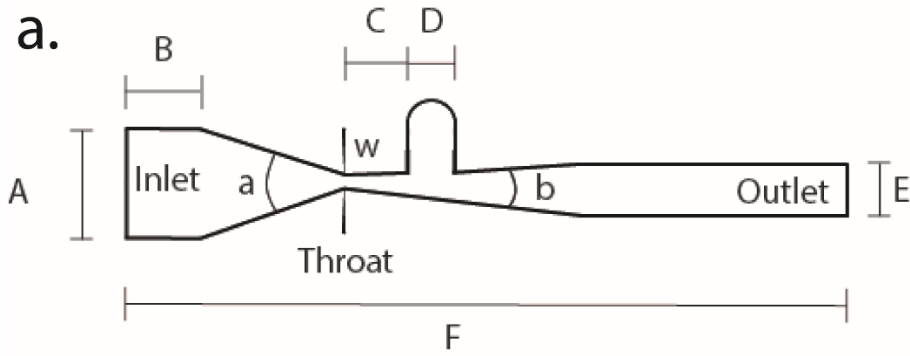
Ahrar, S., Hwang, M., Duncan, P.N., and Hui, E.E. (2013). Microfluidic serial dilution ladder. *Analyst* 139, 187–190.

Bird, R.B. (2002). Transport phenomena. *Appl. Mech. Rev.* 55, R1–R4.

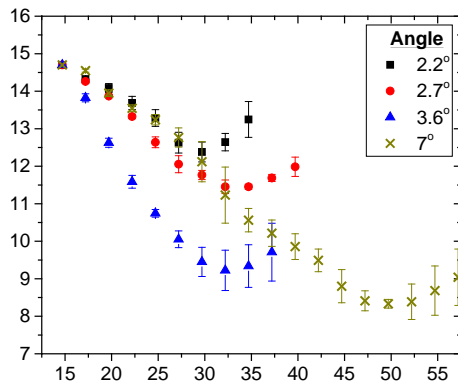
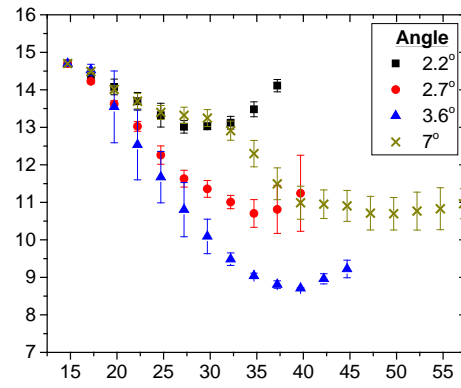
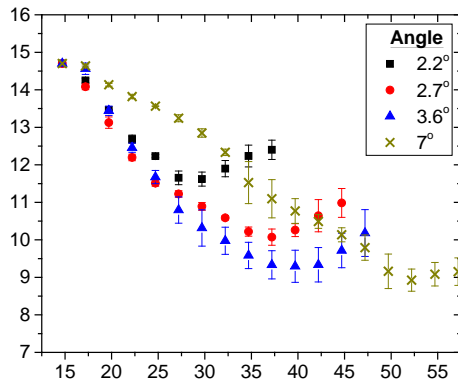
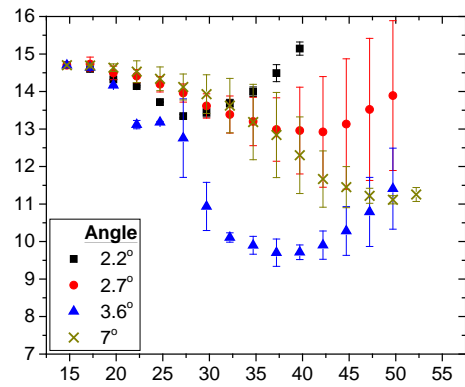
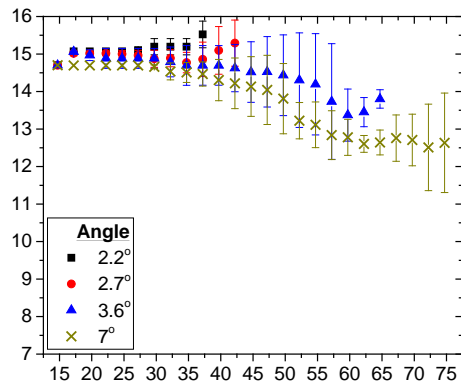
Chang, D.S., Langelier, S.M., and Burns, M.A. (2007). An electronic Venturi-based pressure microregulator. *Lab. Chip* 7, 1791–1799.



- Chang, D.S., Langelier, S.M., Zeitoun, R.I., and Burns, M.A. (2010). A Venturi microregulator array module for distributed pressure control. *Microfluid. Nanofluidics* 9, 671–680.
- Curtis, C., Eshaque, B., Badali, K., and Karanassios, V. (2012). Rapid prototyping of a microfluidics-based Venturi micropump imprinted on polymeric, postage-stamp-sized chips. p. 83660P–83660P–8.
- Duncan, P.N., Nguyen, T.V., and Hui, E.E. (2013). Pneumatic oscillator circuits for timing and control of integrated microfluidics. *Proc. Natl. Acad. Sci.* 110, 18104–18109.
- Duncan, P.N., Ahrar, S., and Hui, E.E. (2015). Scaling of pneumatic digital logic circuits. *Lab. Chip* 15, 1360–1365.
- Gervais, T., El-Ali, J., Günther, A., and Jensen, K.F. (2006). Flow-induced deformation of shallow microfluidic channels. *Lab. Chip* 6, 500–507.
- Grover, W.H., Skelley, A.M., Liu, C.N., Lagally, E.T., and Mathies, R.A. (2003). Monolithic membrane valves and diaphragm pumps for practical large-scale integration into glass microfluidic devices. *Sens. Actuators B Chem.* 89, 315–323.
- Grover, W.H., Ivester, R.H.C., Jensen, E.C., and Mathies, R.A. (2006). Development and multiplexed control of latching pneumatic valves using microfluidic logical structures. *Lab. Chip* 6, 623–631.
- Jensen, E.C., Grover, W.H., and Mathies, R.A. (2007). Micropneumatic Digital Logic Structures for Integrated Microdevice Computation and Control. *J. Microelectromechanical Syst.* 16, 1378–1385.
- Kirby, B.J. (2010). *Micro- and Nanoscale Fluid Mechanics: Transport in Microfluidic Devices* (Cambridge University Press).
- Koo, K., Lee, S., and Cho, D.D. (2011). Fabrication of a Micro-Fluid Gathering Tool for the Gastrointestinal Juice Sampling Function of a Versatile Capsular Endoscope. *Sensors* 11, 6978–6990.
- Li, D., Ji, Y., Liang, W., Zhang, X., Yu, H., and Xu, K. (2013). A portable instrument for continuous glucose monitoring by the integration of microfluidic chip and micro-glucose sensor. pp. 861519-861519–11.
- Nguyen, T.V., Duncan, P.N., Ahrar, S., and Hui, E.E. (2012). Semi-autonomous liquid handling via on-chip pneumatic digital logic. *Lab. Chip* 12, 3991–3994.
- Perdigones, F., Luque, A., and Quero, J.M. (2010). PDMS microdevice for precise liquid aspiration in the submicroliter range based on the Venturi effect. *Microelectron. Eng.* 87, 2103–2109.
- Shapiro, A.H. (1953). The dynamics and thermodynamics of compressible fluid flow.
- Yu, H., Li, D., Roberts, R.C., Xu, K., and Tien, N.C. (2012). Design, fabrication and testing of a micro-Venturi tube for fluid manipulation in a microfluidic system. *J. Micromechanics Microengineering* 22, 35010.

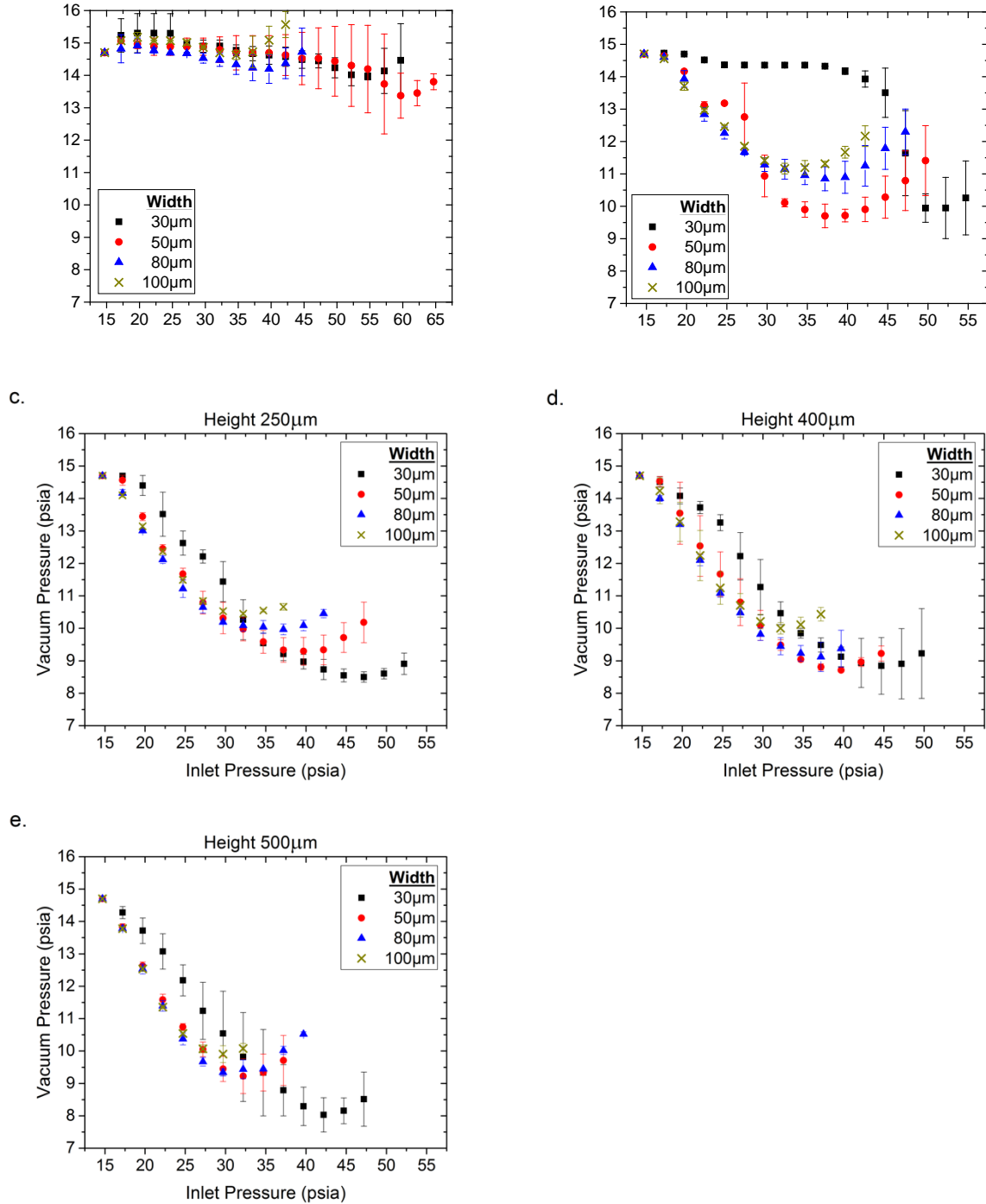


**Figure 1. a.** Schematic of the micro fabricated CD nozzle geometry and the parameters investigated in this study. A converging and a diverging nozzle meet at the throat. Nitrogen is introduced in the converging part and exits on the diverging part. Vacuum pressure is generated at the throat. **b.** The experimental setup. Nitrogen provided by a cylinder is introduced to a pressure regulator and fed into the inlet of the converging diverging nozzle. The inlet pressure and the vacuum pressure are measured by pressure sensors connected to a data acquisition system and processed on a personal computer.



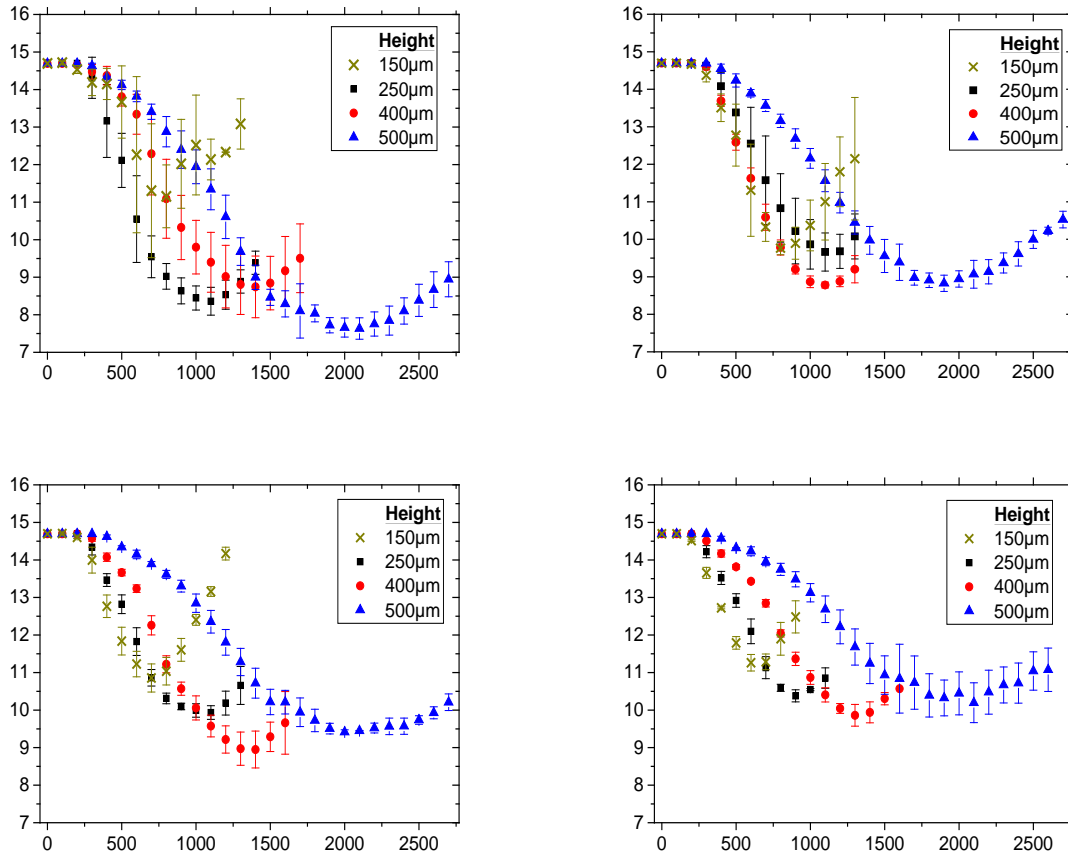
**Figure 2.** Vacuum generated by micro fabricated converging diverging nozzles with throat width of 50µm for different angles of the diverging section and for height of (a) 80µm (b) 150µm (c) 250µm (d) 400µm

and (e) 500 $\mu\text{m}$ . It is observed that the acquired vacuum is limited at small angles of the diverging section and at small heights of the device.

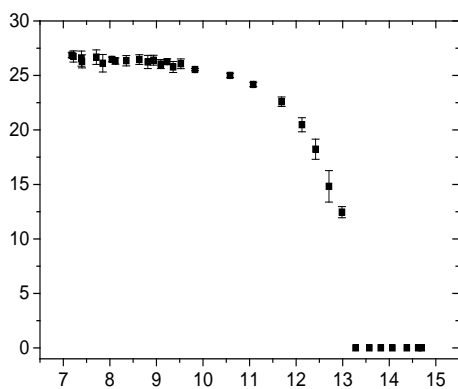
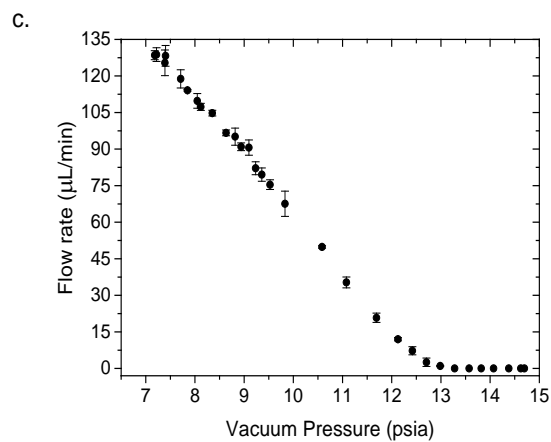
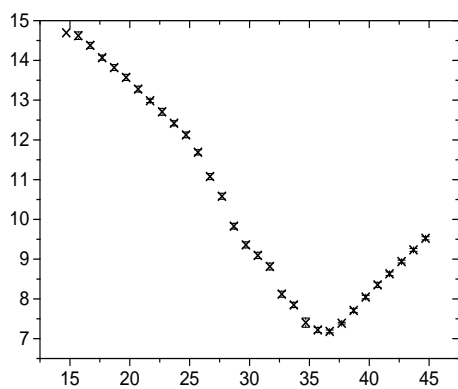
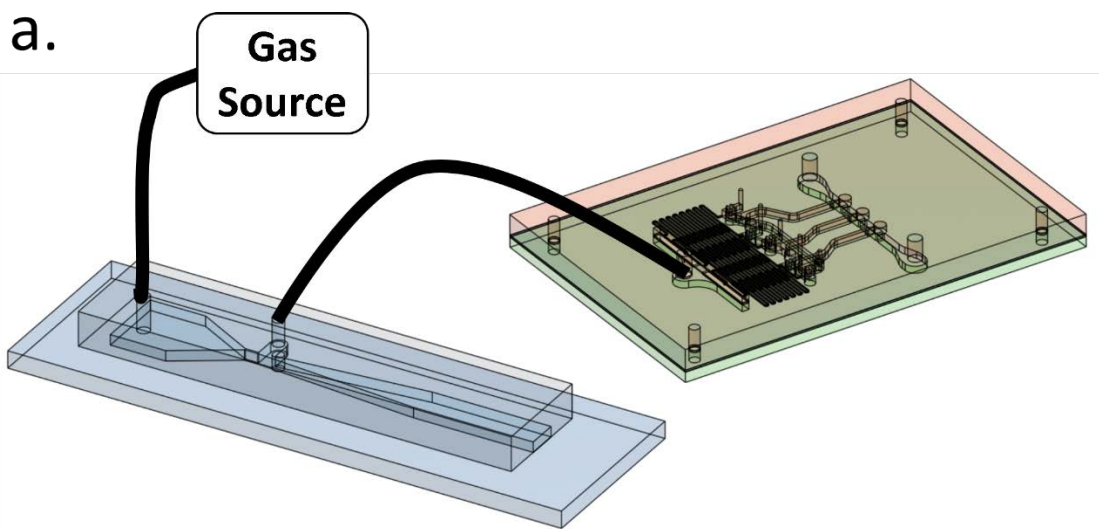


**Figure 3.** Vacuum generated by micro fabricated converging-diverging nozzles with a diverging angle of 3.6° for different throat widths and height of (a) 80 $\mu\text{m}$  (b) 150 $\mu\text{m}$  (c) 250 $\mu\text{m}$  (d) 400 $\mu\text{m}$  and (e) 500 $\mu\text{m}$ .

It is observed that wider throats width generate less vacuum. This observation halts at heights smaller than 150 $\mu\text{m}$ .

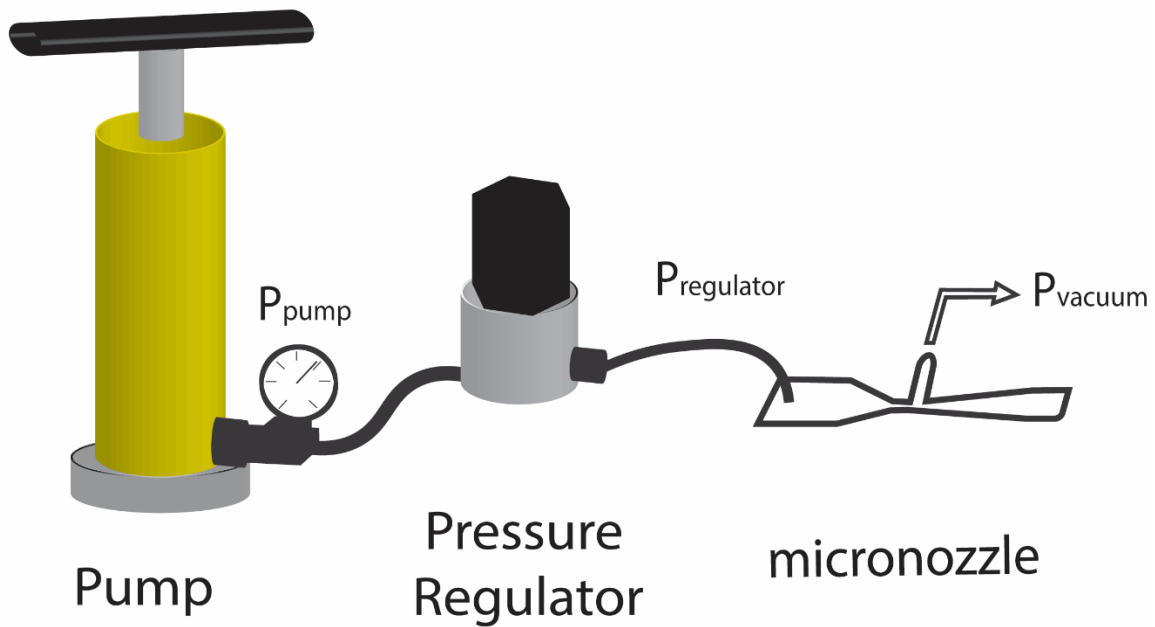


**Figure 4.** Volumetric flow rate of the converging-diverging microfabricated nozzles of 3.6° angle of the diverging part and the acquired vacuum pressure for different heights for different throat widths of (a) 30 $\mu\text{m}$ , (b) 50 $\mu\text{m}$ , (c) 80 $\mu\text{m}$  and (d) 100 $\mu\text{m}$ . It is observed that nozzles with high heights require mostly high volumetric flow rates for the same vacuum pressure to be obtained but enable lower vacuum pressures to be achieved.



**Figure 5. a.** Micropump-micronozzle integration. Gas source (air tank, pump, or house air) provides positive pressure, which is converted to vacuum by the micronozzle to drive the pneumatic logic pump. **b.** Generated vacuum pressure as a function of input pressure. Diverging nozzle angle =  $3.6^\circ$ , throat width =  $30\mu\text{m}$ , and height =  $500\mu\text{m}$ . **c.** Pump flow rate as a function of vacuum pressure. **d.** Oscillation frequency of the pump as a function of vacuum pressure.

a.



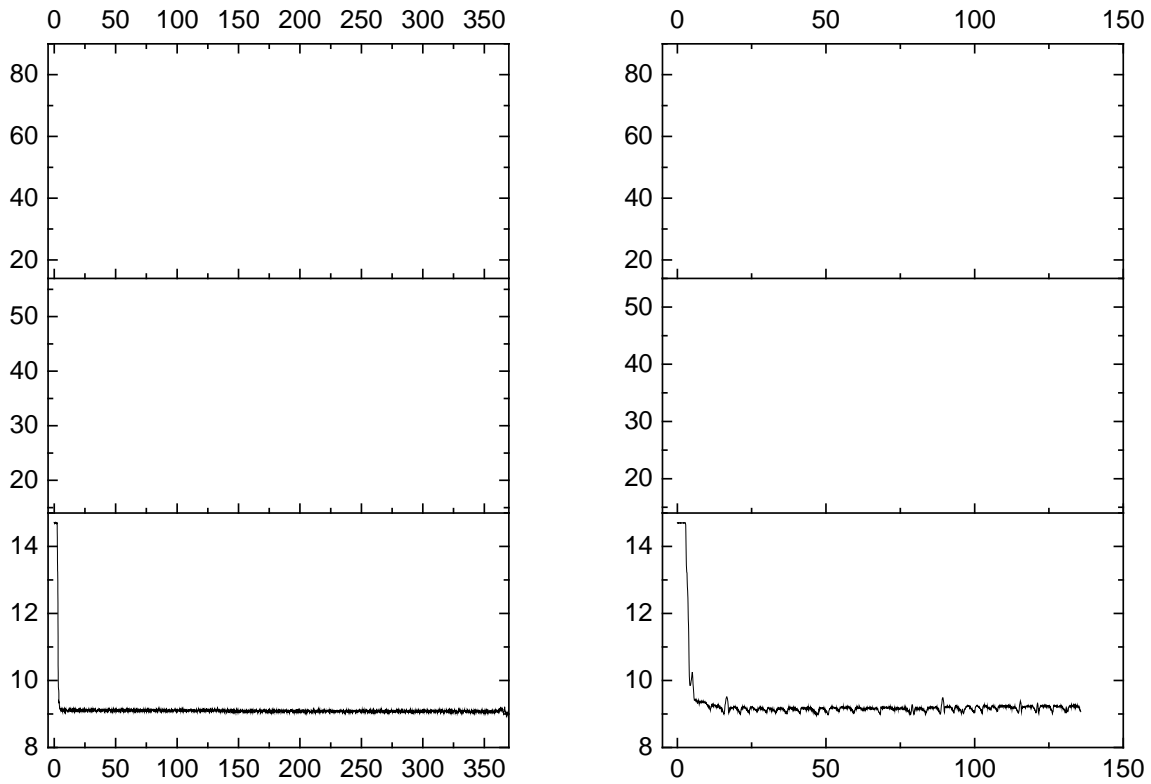


**Figure 6. a.** Use of bike pump to power converging-diverging nozzle to produce vacuum pressure. The pressure is stabilized by using a pressure regulator. **b.** Pump, inlet and the acquired vacuum pressure of the micronozzle of the suggested setup of a bike pump as shown in figure 6. The throat width of the micronozzle is  $30\mu\text{m}$ , the height is  $500\mu\text{m}$  and the angle of the divergent part is  $3.6^\circ$ . A stable vacuum pressure of  $9.09\text{psia}$  within a range of  $0.11\text{psi}$  was produced for about 6 minutes by providing to the micronozzle an inlet pressure of  $53.4\text{psia}$  within a range of  $1.48\text{psi}$ . In figure 6c, it is evident that the inlet pressure drops if the pressure of the pump is less than the pressure set by the pressure regulator.



## Supplement

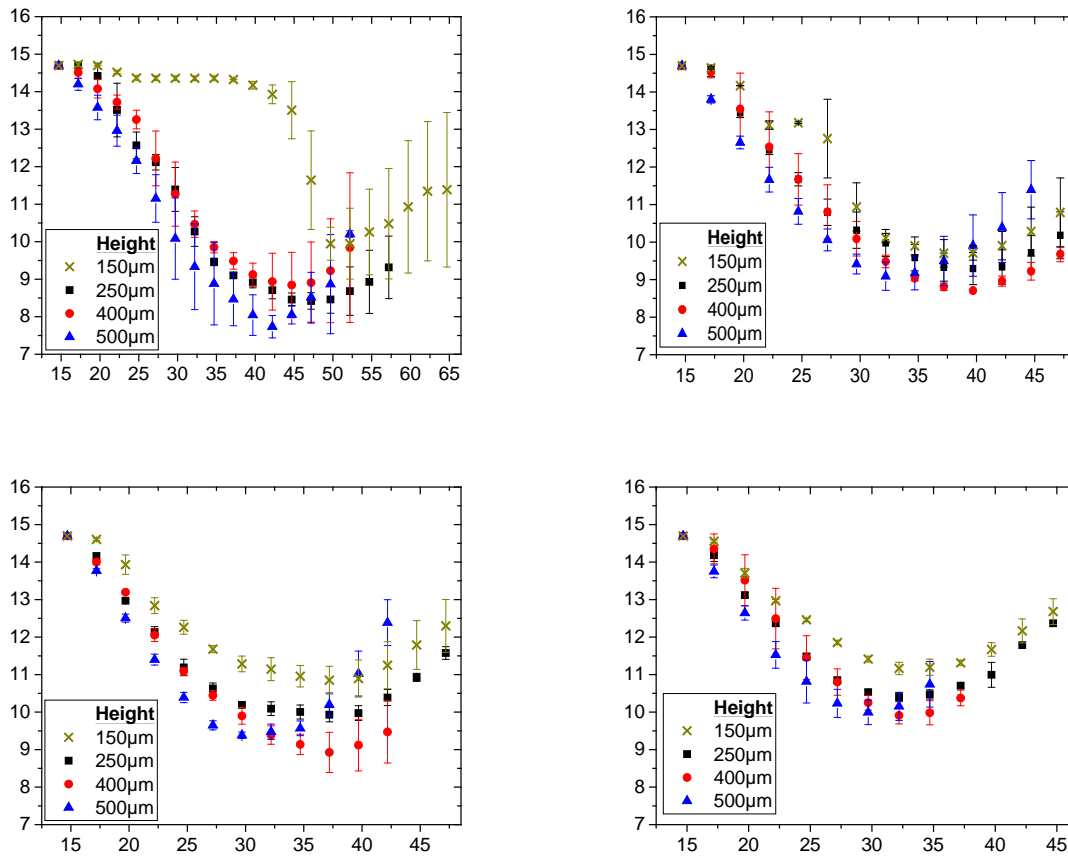


**Figure S1.** Inlet pressure of the converging-diverging microfabricated nozzles of  $3.6^\circ$  angle of the diverging part and the acquired vacuum pressure for different heights and of different throat width of (a)  $30\mu\text{m}$  (b)  $50\mu\text{m}$  (c)  $80\mu\text{m}$  and (d)  $100\mu\text{m}$ . It is observed that the wider the throat width the less vacuum is obtained. This observation halts at heights smaller than  $150\mu\text{m}$ .

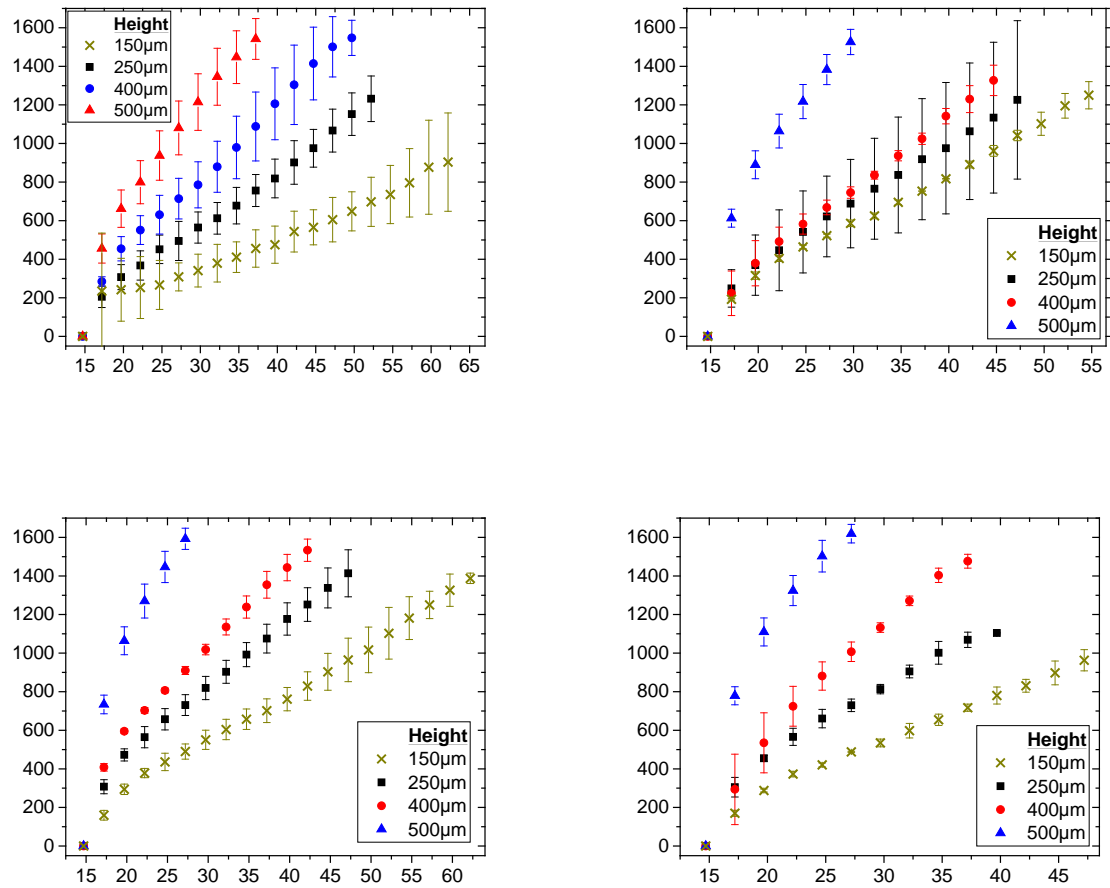


**Figure S2.** Volumetric flow rates for different inlet pressures of the converging-diverging microfabricated nozzles of  $3.6^\circ$  angle of the diverging part and the acquired vacuum pressure for different heights and different throat width of (a)  $30\mu\text{m}$  (b)  $50\mu\text{m}$  (c)  $80\mu\text{m}$  and (d)  $100\mu\text{m}$ . It is observed that the wider the throat width the less vacuum is obtained. This observation halts at heights smaller than  $150\mu\text{m}$ .